

The Study of Post-Harvest Processing and Handling of Residues From Plants Grown Primarily For Agronomics: Soybean Stalk, Corn Stover, Tomato Vine, Cucumber, Eggplant, and Summer Squash

Omid Gholami Banadkoki^{1,2,*}, Shahab Sokhansanj^{1,2}, Anthony Lau^{1,2}, Jun Sian Lee^{1,2}, Selvakumari Arunachalam³, and Donald Smith³

ABSTRACT

Information on post-harvest handling of the crop is critical to the development of new or improved plant species and traits. This paper presents a comprehensive study of the grinding characteristics and handling properties of a number of crop residues under agronomic studies. We used a laboratory-scale knife mill connected to an in-line power meter to investigate the specific energy of size reduction for each crop. The summer squash sample yielded the smallest mean particle size upon grinding ($P = 0.05$). The results indicate a significant correlation between the Carbon to Oxygen (C/O) ratio and the Gross Calorific Value (GCV), ash, lignin content, and net specific grinding energy consumption (NSGEC) of the samples. Among agricultural residues, the soybean stalk sample, with the highest C/O ratio (0.96), exhibited the highest GCV (17.5 MJ/kg, db) and NSGEC (31.7 kWh/t), while the summer squash sample, with the lowest C/O ratio (0.46), showed the lowest GCV (13.6 MJ/kg, db) and NSGEC (5.1 kWh/t). The flowability of the ground biomass samples varied, with cucumber showing the best free flow properties. The results also showed that there is a significant positive correlation between the lignin content and NSGEC of all samples ($p = 0.05$).

Submitted: August 21, 2024

Published: October 23, 2024

 10.24018/ejfood.2024.6.5.859

¹Biomass and Bioenergy Research Group (BBRG), University of British Columbia, Canada.

²Chemical and Biological Engineering Department, Faculty of Applied Science, University of British Columbia, Canada.

³Plant Science Department, Faculty of Agricultural and Environmental Science, McGill University, Canada.

*Corresponding Author:

e-mail: omid1370@mail.ubc.ca

Keywords: Biomass feedstock, Particle size, Physicochemical properties, Specific grinding energy.

1. INTRODUCTION

The recent challenges in developing a more sustainable energy supply to mitigate GHG emissions, coupled with increasing global demand for food as a consequence of population growth, have led to intensified agricultural activities and the generation of agricultural residues [1]. Although Canada has enormous volumes of wheat, access to this straw is un-economical and requires long-distance transport with an intensive environmental footprint. Non-traditional biomass, like horticultural crops, may provide new sources of biomass. In 2022, 0.8 million tons of tomato vines, which have a considerable number of lignocellulosic components, will be produced in Canada [2], [3]. The residue from tomato crops has been recognized as a promising and sustainable lignocellulosic material for

producing both native cellulose microfibrils (CMF) and functionalized cellulose nanocrystals (CNC) [4]. Harvesting soybeans resulted in approximately 22.4 million tons of crop residue in Canada in 2022 [5]. Soybean residue is an abundant source of cellulosic microfibrils (SMF) and brick-like microparticles (SMP) with higher amounts of hemicellulose content, higher crystallinity, and thermal stability, which makes it an attractive option to reinforce thermoplastic composites [6].

A successful conversion of lignocellulosic biomass into valuable products hinges on effective size reduction [7]–[9]. For instance, the proper particle size for pelletizing ranges from 0.6–0.87 mm [10], [11], for gasification ranges from 0.2–1.5 mm [12], [13], for anaerobic digestion 50–750



microns [14], and recommended particle size for pyrolysis ranges 0.25 mm–2 mm [15], [16].

The three most common grinding mills are hammer mills, knife mills, and ball mills. Different grinding methods for biomass have been compared to highlight the influence of the device type on energy consumption and particle size distribution [17], [18]. Using knife mill for Douglas fir chips consumed higher energy and resulted in smaller particle size in comparison with hammer mill [19]. Knife mill was particularly effective for fibrous agricultural residues [17].

Higher lignin content often results in greater resistance to size reduction processes, affecting both the specific grinding energy and particle size distribution [9]. Investigations on the effect of lignin content showed that softwood sawdust samples with higher lignin content had less specific grinding energy [20]. In contrast, another research comparing cellulose and lignin content of sawdust samples and agricultural straws stated that the higher specific energy grinding is associated with a higher amount of cellulose and lignin [9].

The Gross Calorific Value (GCV) represents the maximum energy released during complete combustion [21]. GCV is essential for evaluating biomass energy content [22] and optimizing process parameters for conversion technologies like combustion, gasification, or pyrolysis [23]. GCV varies significantly based on feedstock type, moisture content, and other elemental and compositional factors [24]. The C/O ratio in biomass properties, representing the carbon-to-oxygen ratio, is a key metric for evaluating the chemical composition, stability and reactivity, thermal properties, hydrophobicity, and quality of biomass [25].

Generally, lower moisture and higher carbon content contribute to a higher GCV [26]. The ash content refers to the inorganic residue left after biomass combustion [21]. High ash content presents challenges such as equipment fouling and corrosion during combustion, impacting bio-fuel quality and thermal conversion efficiency [27]. The ash content varies with different particle sizes, with a higher amount of ash content concentrated in the fine particles [28]. The reduction in ash content leads to an increase in gross calorific value [29], [30]. Materials with higher moisture content have higher specific grinding energy and poorer flowability behavior [31]–[34].

Machine vision, as an advanced technique, has been used by researchers to examine particle size and shape through images [35]–[38]. ImageJ is an open-source image processing software that can be used to extract quantitative data from images and precisely characterize particle dimensions and morphological features. This approach offers a highly efficient and accurate means of features like length, width, area, perimeter, aspect ratio, roundness, and circularity [39], [40]. The relationship between particle shape and size distribution and flowability for efficient handling and transportation of biomass have been examined by researchers [32], [37], [40]–[42]. Ground particles with higher sphericity, roundness, and circularity had better flowability [40]. An investigation of the AOR in different size fractions proved that smaller particle size was

associated with better flowability [42]. In general, flowability is associated with smaller particles, higher aspect ratios, and highly spherical particles [31], [32], [39], [43], [44].

The flowability of particles is also intricately linked to various properties such as particle density, bulk density, Hausner ratio, and AOR [31], [45]. Bulk density is a key factor in determining the flow behavior of a material, with higher bulk densities generally associated with better flowability [46]. The Hausner ratio provides quantitative measures of powder flow properties, where higher values indicate reduced flowability [47]. The angle of repose is another indicator of flowability, where higher AOR is associated with lower flowability [47].

1.1. Objectives

Agronomists are not only tackling challenges related to crop performance and stress management but are equally invested in assessing the post-harvest characteristics of the biomass portion of emerging crop strains for bioenergy and bioproduct applications. The primary step in the processing of biomass is size reduction with respect to energy input and particle size distribution of the biomass. The experimental data encompasses a range of critical compositional and physical properties of the ground biomass that are critical to the efficient handling and processing of the biomass.

2. MATERIALS AND METHODS

Corn, soybean, tomato, cucumber, eggplant, and summer squash were cultivated and harvested either in greenhouses or on experimental plots in Plant Science Department of McGill University, Montreal in 2021. Sawdust from lodgepole pine and white spruce with 50/50 split, was supplied by Premium Pellet Co., Vanderhoof, British Columbia, as the commercial baseline material for comparison purpose. The samples had 5%–10% (wet mass basis) moisture content as received.

Fig. 1 shows corn stover samples consisting of large pieces of stalks and leaves. The soybean stalk samples included brittle stems and shriveled leaves. The eggplant biomass was mainly composed of crushed leaves and some thick and long wooden stems. Tomato vine is comprised of wooden stems and some chopped leaves. The bush-like cucumber and summer squash samples had thin, brittle stems and crushed leaves. Sawdust was taken at the pellet plant before grinding. The samples were kept in air-tight bags to minimize moisture uptake.

Samples were ground using a knife mill (Model SM100, Retsch Inc., Newtown, PA) having a screen with square perforations of 4 mm. After recording the initial mass, the as received biomass samples were fed by hand into the infeed chute. The time of feeding was recorded using a digital timer. An in-line HOB0 Plug Load Data Logger (Model UX120-018, Onset HOB0, USA) was used to measure and record instantaneous power data at 1 second intervals. Ground samples were collected and stored in air-tight bags for further testing.



Fig. 1. Pictures of the as-received biomass samples cultivated and harvested in an experimental greenhouse at McGill University.

Samples were ground in four replications, and the power consumption data were logged for each replicate to calculate the net-specific grinding energy consumption. Fig. 2 shows a typical record of a grinding cycle. In this particular test, the sample was fed into the grinder gradually 14 times. The red line in Fig. 2 represents the grinder power consumption under no-load conditions. There is no considerable fluctuation in power while the grinder is empty ($P_{no-load} = 484.4$ W). The blue line shows instantaneous power consumption at 1 second intervals. There were large fluctuations in the power during operation as the samples were fed manually into the grinder. The small peaks (in the range of 550–650 W) are associated with the power use response to the feeding step. The larger peaks (in the range of 650–950 W) are related to pressing the samples into the grinding chamber using the wooden plunger after each feed cycle. The data logger unit recorded the power of grinding (dP) over each time step of one second (dt). The total specific grinding energy consumption (TSGEC) is presented as the sum of instantaneous power recorded every second during the grinding process. The net specific grinding energy consumption (NSGEC) is the difference between the TSGEC and the energy required to run the grinder under a no-load condition [33], [34], [39].

The following equations are used to convert power to energy and calculate specific energy.

$$E_{Net}(kJ) = E_{Load}(kJ) - E_{No-Load}(kJ)$$

$$= \sum_{t=0}^n d(P_{Load} - P_{No-Load}) \times dt \quad (1)$$

$$NSGEC \left(\frac{kWh}{t} \right) = \frac{E_{Net}(kJ)}{m(kg) \times 3.6} \quad (2)$$

where E_{Load} is energy consumption in kJ while samples were loaded in grinder, $E_{No-Load}$ is energy consumption of the grinder in kJ while no sample was loaded, P_{Load} is the power consumption in Volts-Amps while samples were loaded in grinder, $P_{No-Load}$ is the power consumption of the grinder in Volts-Amps while no sample was loaded in grinder, dt is the time intervals of the data logger, E_{Net} is the net energy consumption in kJ, m is the mass of the samples in kg loaded into the grinder, and $NSGEC$ is the Net Specific Grinding Energy Consumption of the samples in kWh/t.

The particle size distribution was conducted by sieving in accordance with the ANSI/ASAE standard S319.4 (ASAE, 2008b). Roughly 100 g of the sample was placed on top of a stack of sieves on a Ro-Tap shaker (Tyler Industrial Products, Cleveland, OH). The selected sieve sizes were 4, 2, 1.18, 0.5, 0.25, and 0.125 mm. The shaker

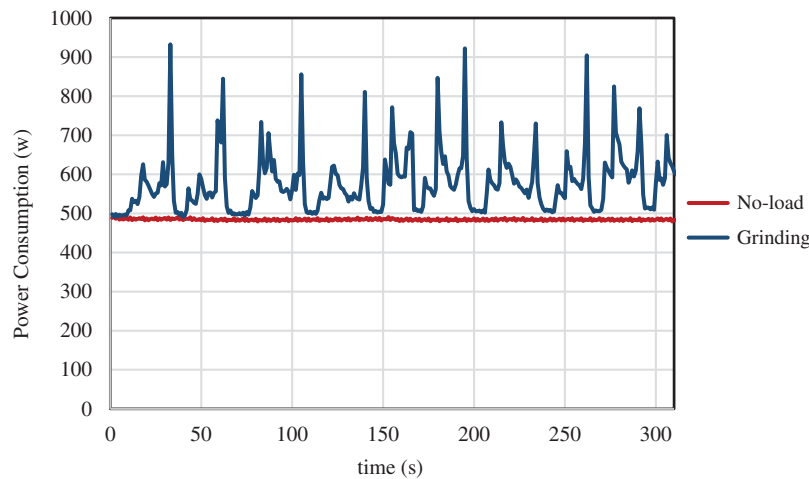


Fig. 2. Energy consumption in No-load and Grinding condition. Difference between No-load and Grinding condition represents the net specific grinding energy consumption (NSGEC).

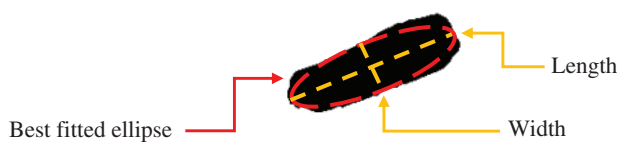


Fig. 3. Determining best fitted ellipse to obtain width (W), length (L), area (A), and perimeter (P).

subjects the contents of the sieve to oscillation motions and tapping for 10 minutes. The mass retained on each sieve and in the pan was weighed on an electronic balance to 0.01 g precision. All particle size distribution was measured in four replications. Calculation of particle size, surface area, and number of particles by mass calculations assumes that particle sizes of all ground material are logarithmic-normally distributed.

The shape factors of the particles were determined through image processing using the open-source software, ImageJ (Version 1.53K, National Institutes of Health, USA). A sample of 100 particles were taken randomly from each samples and were photographed using a cell-phone camera. Fig. 3 shows the determination of best fitted ellipses on particles to obtain width (W), length (L), area (A), and perimeter (P).

Aspect ratio (AR) is defined as the ratio of the width to length of the particle and is calculated using Eq. (3) [40], [44], [48]. Aspect ratio is a dimensionless parameter, and it varies from 0 to 1.

$$AR = \frac{W}{L} \quad (3)$$

The specific particles density is measured using a gas pycnometer (Quantachrome Instruments, Boyton Beach, FL, USA; Model MVP-D160-E). All specific density measurements are repeated five times to achieve the reproducibility of the results.

The bulk density of loose and dense materials was determined as the ratio of mass over aerated volume. The tapped bulk density was obtained upon tapping the volume of the material against a padded bench top 50 times (sufficient taps to make sure there is no change in the volume anymore).

The Hausner Ratio (HR) that is an indicator of the flowability of the ground material, is calculated by dividing the tapped bulk density over the loose bulk density. HR is a dimensionless index [39], [47].

The Angle of Repose (AOR) is one of the indexes to evaluate the flowability of particles. AOR is the angle of piled particles with respect to the horizontal surface. AOR depends on the particle size, particle shape, cohesiveness, and stickiness of particles [49]. It is suggested that an AOR below 30° shows good flowability, 30°–45° some cohesiveness, 45°–55° true cohesiveness and above 55° very high cohesiveness [49].

The moisture content of the samples was analyzed according to ASABE S358.2 (2010) and by using a convection oven at 105°C for 24 hours. The measurements were done with four replications and reported on a wet basis.

The ash content of ground samples was measured with four replications [50]. Ash content was determined as the percentage of residue remaining after dry oxidation at 550°C–600°C in a furnace.

The Gross Calorific Value (GCV) was determined by an oxygen bomb calorimeter (Parr Model 6100) using ASTM standard D-2015.

The extractives of ground material were measured in dry basis using a Soxhlet unit [51].

The lignin content of ground material was analyzed in four replications for insoluble (Klason) lignin contents [51]. All extractive and lignin measurements are repeated four times to confirm the reproducibility of data.

The elemental analysis of the ground samples was measured via FISONs-EA 1108 (Thermo Fisher Scientific, USA) Elemental Analyzer in 4 replicates.

3. RESULTS AND DISCUSSION

3.1. Grinding Observations

The sample of con stover and leaves exhibited considerable resistance to grinding due to the spongy and elastic nature of their stalks. The brittleness of the tomato vines led to the easiest grinding among all samples. Grinding tomato vines and eggplant samples resulted in the highest amount of dust generated, while sawdust produced



Fig. 4. Grinding chamber after grinding. Grinding leftovers represents the plugging of the screen.

the least during the process. The slenderness and brittleness bush-type of cucumber and summer squash samples resulted in the least resistance to grinding. Upon cessation of the in-flow, most of the samples were successfully cleared from the grinder cavity. However, an exception was noted with corn stover, summer squash, and eggplant samples, where significant amounts of materials remained within the cavity (Fig. 4). This accumulation of these samples led to an overcurrent situation, highlighting the unique challenges posed by their mechanical strength during the grinding process.

3.2. Material and Power Input to Grinder

Table I lists the mass and energy flows for the grinding tests. The moisture content ranges from 6.2% for corn stover to 10.2% for cucumber, representing a long-term equilibrium in laboratory conditions. Mass fed to the grinder varies depending on the biomass crop, reflecting the availability of biomass for testing. The disparity between mass inflow and outflow denotes material loss during grinding. Feeding time correlates with the amount of biomass tested. Net grinding energy is computed using (1) and (2).

3.3. Particle Size Analysis

Fig. 5 shows cumulative distribution of particles size with respect to sieve opening size. Ground ag-residue samples had a considerable amount of fine particles (below 125

microns) in comparison with commercial sawdust samples. Summer squash has a sharper increase in the cumulative weight percentage at smaller sieve sizes, demonstrating it has the highest amount of fine particles among all samples. The curves for cucumber, tomato vine, and eggplant show a moderate slope than summer squash (about 10% fine particles), indicating they have relatively a higher proportion of smaller particles. The cumulative distribution curve of corn stover and soybean stalk displays a moderate slope (about 5% fine particles), suggesting a more balanced distribution of particle sizes. The sawdust sample has a more gradual cumulative size distribution curve compared to all agricultural byproducts.

Fig. 6 shows the distribution of particle size specifying the mean particles size D50, D16, and D80. D80 represents that 80% of the particles are below the size on vertical axis. The result of the mean particle size analysis shows that all tested agricultural residues have significantly smaller particles compared to sawdust samples after grinding. Among agricultural residues, the ground summer squash and tomato vine samples show the lowest values for all particle sizes. The smaller particles are difficult to handle.

3.4. Particle Shape Analysis

Fig. 7 presents the results of the particle shape analysis of ground samples. A higher aspect ratio indicates a more circular particle. The highest aspect ratio belongs to eggplant (0.45), and the lowest value is associated with the cucumber and corn stover (0.32) (Fig. 7). This indicates that ground corn stover and cucumber particles are more elongated compared to the others. The aspect ratios of corn stover, soybean stalk, cucumber, and sawdust samples do not show any significant difference ($P = 0.05$). Also, there is no considerable difference between the aspect ratio of eggplant, summer squash, and tomato vine samples ($P = 0.05$). This suggests that these biomasses have similar elongation characteristics, flow behavior, and mechanical interlocking during downstream processes like storage and pelletization.

3.5. Elemental Analysis

The results of the elemental analysis of the ground biomass are depicted in Table II. Sawdust sample considerably has the highest (50.39 %) carbon content and lowest (45.53%) oxygen content among all samples. The highest and lowest oxygen content belongs to summer squash (63.8%) and soybean stalk (47.75%), respectively. Conversely, the summer squash and soybean stalks have the lowest (29.02%) and highest (46.04%) carbon content.

TABLE I: MASS IN-FLOW AND ENERGY CONSUMPTION OF THE KNIFE MILL TO CALCULATE THE PERFORMANCE OF THE KNIFE MILL GRINDER

| Samples | Moisture content (wb, %) | Pre-grind mass (g) | Post-grind mass (g) | Feeding time (s) | Feeding rate (g/s) | Net energy (kJ/kg) |
|---------------|-----------------------------|--------------------|---------------------|------------------|--------------------|--------------------|
| Corn stover | 6.2 | 500.6 | 486.6 | 503 | 0.97 | 89.4 |
| Soybean stalk | 7.5 | 537.4 | 519.0 | 746 | 0.70 | 114.1 |
| Tomato vine | 8.6 | 660.9 | 622.2 | 372 | 1.68 | 50.7 |
| Eggplant | 10.0 | 1147.0 | 1129.6 | 459 | 2.48 | 32.4 |
| Cucumber | 10.2 | 184.7 | 173.5 | 153 | 1.16 | 44.3 |
| Summer squash | 9.7 | 533.0 | 545.1 | 240 | 2.26 | 18.2 |
| Sawdust | 9.7 | 121.5 | 104.5 | 261 | 0.41 | 278.1 |

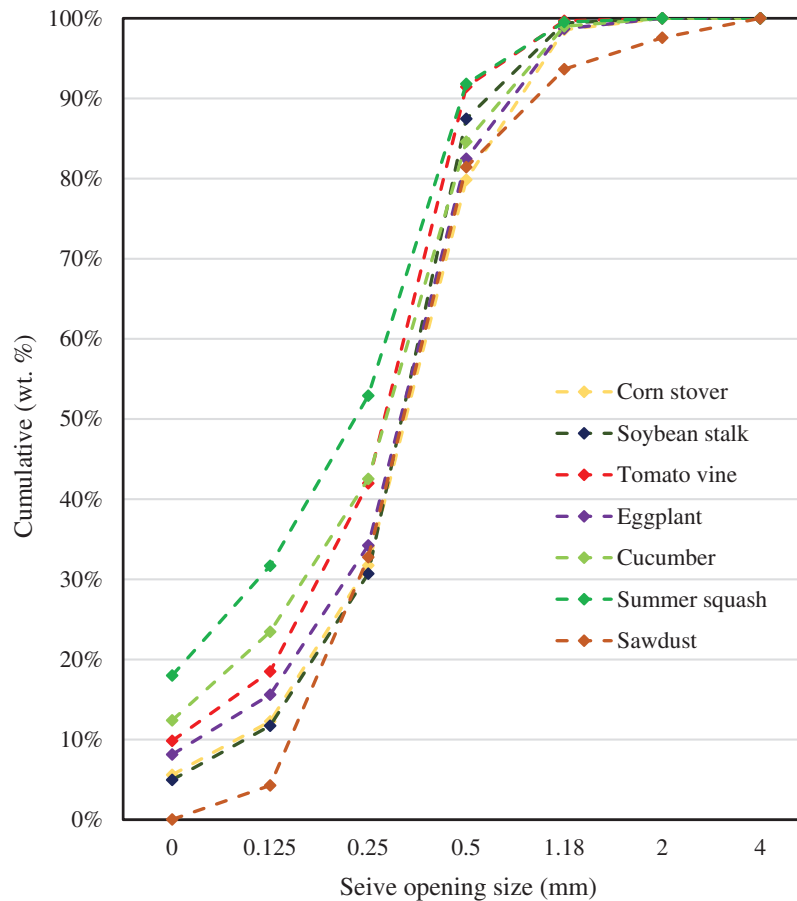


Fig. 5. Cumulative particle size distribution of corn stover, soybean stalk, tomato vine, eggplant, cucumber, summer squash, and sawdust sample according to ANSI/ASAE standard S319.4 (ASAE, 2008b).

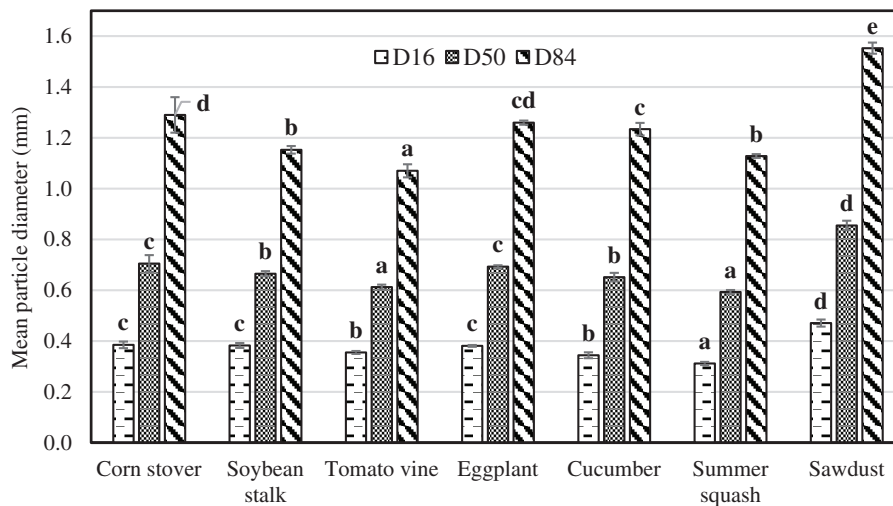


Fig. 6. Mean particle size of the ground corn stover, soybean stalk, tomato vine, eggplant, cucumber, summer squash and sawdust.

3.6. Physio-Chemical and Structural Components

The results of the physio-chemical, structural components, and the net specific grinding energy consumption (NSGEC) of the samples are listed in Table III. The sawdust sample exhibits the highest GCV (21.0 MJ/kg, db) and the lowest ash content (0.3%). Among the agricultural residues, summer squash has the lowest GCV (13.6 MJ/kg, db) and the highest ash content (33.6%). Conversely, the highest GCV (17.6 MJ/kg, db) and the lowest ash content (5.7%) belong to the corn stover sample. The primary factor influencing these variations in GCV and ash content

is the Carbon to Oxygen (C/O) ratio. According to the Pearson correlation matrix (Table IV), there is a significant positive correlation between the C/O ratio and GCV; conversely, there is a significant negative correlation between the C/O ratio and the ash content of all samples.

Similarly, lignin content is positively correlated to the C/O ratio (Table IV). The highest lignin content belongs to sawdust sample (29.2%) with the highest C/O ratio (1.16). In a contrary trend, the lowest lignin content (5.6%) belongs to the summer squash sample with the lowest C/O ratio (0.46).

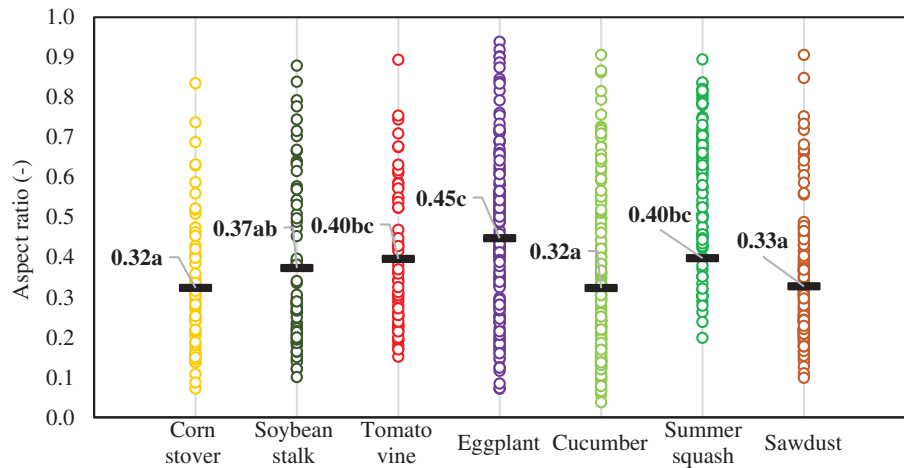


Fig. 7. Aspect ratio of the ground corn stover, soybean stalk, tomato vine, eggplant, cucumber, summer squash and sawdus.

TABLE II: ELEMENTAL ANALYSIS OF GROUND CORN STALKS, SOYBEAN STALKS, TOMATO VINES, EGGPLANT, CUCUMBER, SUMMER SQUASH, AND SAWDUST SAMPLE

| Samples | C% | N% | H% | S% | O% |
|----------------|---------|---------|---------|---------|---------|
| Corn stover | 45.79 d | 0.50 b | 5.66 d | 0.00 a | 48.05 b |
| Soybean stalk | 46.04 d | 0.47 b | 5.75 d | 0.00 a | 47.75 b |
| Tomato vine | 41.28 c | 1.17 c | 5.21 c | 0.40 b | 51.95 d |
| Eggplant | 41.62 c | 2.89 d | 5.27 c | 0.39 b | 49.84 c |
| Cucumber | 35.68 b | 3.27 e | 4.71 b | 0.50 d | 55.85 e |
| Summer squash | 29.02 a | 2.82 d | 3.91 a | 0.45 c | 63.80 f |
| Sawdust | 50.39 e | 0.00 a | 6.08 e | 0.00 a | 43.53 a |
| Pr > F (Model) | <0.0001 | <0.0001 | <0.0001 | <0.0001 | <0.0001 |
| Significant | Yes | Yes | Yes | Yes | Yes |

Note: a, b, c, and d; represent the statistical difference by the LS means method.

TABLE III: THE STATISTICAL DIFFERENCE OF MEANS OF PHYSIO-CHEMICAL, STRUCTURAL COMPONENTS, AND NET SPECIFIC GRINDING ENERGY OF CORN STALKS, SOYBEAN STALKS, TOMATO VINES, EGGPLANT, CUCUMBER, SUMMER SQUASH, AND SAWDUST SAMPLE WITH THE METHOD OF LS MEAN

| Samples | GCV (MJ/kg, db) | Ash (%) | C/O ratio | Extractive (%) | Lignin (%) | NSGEC (kWh/t) |
|----------------|-----------------|---------|-----------|----------------|------------|---------------|
| Corn stover | 17.6 d | 5.7 b | 0.95 e | 5.67 c | 15.4 d | 24.8 d |
| Soybean stalk | 17.5 cd | 7.3 c | 0.96 e | 1.49 a | 18.5 f | 31.7 e |
| Tomato vine | 14.8 b | 17.3 e | 0.79 c | 4.79 b | 16.2 e | 14.1 c |
| Eggplant | 16.7 c | 14.5 d | 0.84 d | 4.36 b | 12.4 c | 9.0 b |
| Cucumber | 14.3 ab | 25.3 f | 0.64 b | 1.82 a | 9.4 b | 12.3 c |
| Summer squash | 13.6 a | 33.6 g | 0.46 a | 1.70 a | 5.6 a | 5.1 a |
| Sawdust | 21.0 e | 0.3 a | 1.16 f | 2.17 a | 29.2 g | 77.3 f |
| Pr > F (Model) | <0.0001 | <0.0001 | <0.0001 | <0.0001 | <0.0001 | <0.0001 |
| Significant | Yes | Yes | Yes | Yes | Yes | Yes |

Note: a, b, c, and d; represent the statistical difference by the LS means method.

TABLE IV: PEARSON CORRELATION MATRIX OF THE VARIABLES

| Variables | Lignin (%) | C/O ratio | GCV (MJ/kg, db) | Ash C. (%) | NSGEC (kWh/t) |
|-----------------|------------|-----------|-----------------|------------|---------------|
| Lignin (%) | 1 | | | | |
| C/O ratio | 0.921 | 1 | | | |
| GCV (MJ/kg, db) | 0.893 | 0.921 | 1 | | |
| Ash C. (%) | −0.881 | −0.981 | −0.910 | 1 | |
| NSGEC (kWh/t) | 0.929 | 0.813 | 0.897 | −0.763 | 1 |

Note: Values in bold are different from 0 with a significance level $\alpha = 0.05$.

There is also a significant positive correlation between the NSGEC and the C/O ratio (Table IV). The sawdust sample, with the highest C/O ratio, has the highest NSGEC among all studied materials (77.8 kWh/t). This is an expected result as wood cells basically contain more lignin and cellulose, and their structure and morphology differ

from plant cells [9]. There is also a considerable positive correlation between NSGEC and lignin content. This observation is opposed to the finding of Naimi *et al.* [20]. Among agricultural residues, soybean stalk exhibited the highest net specific grinding energy consumption, nearing 31.9 kWh/t. Conversely, crushing summer squash stems

TABLE V: PHYSICAL AND FLOW PROPERTIES OF THE CORN STOVER, SOYBEAN STALK, TOMATO VINE, AND SAWDUST ACCORDING TO THE CLASSIFICATION METHOD DEVELOPED BY MCGLINCHY IN 2009 [47]

| Samples | Particle density (kg/m ³) | Bulk density (kg/m ³) | Porosity (–) | HR (–) | AOR (°) | Flow class based on angle of repose |
|---------------|---------------------------------------|-----------------------------------|--------------|--------|---------|-------------------------------------|
| Corn stover | 1238.7 a | 107.7 a | 0.913 g | 1.30 b | 44.5 c | Fair flowing |
| Soybean stalk | 1398.5 b | 200.2 d | 0.857 d | 1.35 d | 52.2 f | Cohesive |
| Tomato vine | 1423.7 c | 259.9 e | 0.817 a | 1.29 b | 43.6 c | Fair flowing |
| Eggplant | 1626.8 d | 196.4 c | 0.879 f | 1.33 c | 48.0 d | Cohesive |
| Cucumber | 1700.6 e | 259.5 e | 0.847 c | 1.25 a | 39.9 a | Free Flowing |
| Summer squash | 1798.9 f | 289.0 f | 0.839 b | 1.25 a | 42.0 b | Fair flowing |
| Sawdust | 1395.3 b | 186.9 b | 0.866 e | 1.25 a | 49.7 e | Cohesive |

Note: a, b, c, and d represent the statistical difference by the LS means method. AOR Angle of repose, HR Hausner ratio.

required significantly less energy (5.1 kWh/t). The variability in the energy consumption for size reduction of biomass is ascribed to their biophysical structures and biochemical composition, as these properties determine the material's resistance to fracture under applied stress [9], [52]. The highest NSGEC for sawdust can be attributed to the highest lignin content of this sample, as lignin primarily provides hardness and stiffness in cell structure [9], [53].

3.7. Flowability Classification

Table V summarizes the physical and flow properties of the corn stover, soybean stalk, tomato vine, eggplant, cucumber, summer squash, and sawdust samples. Based on the classification method developed by McGlinchey in 2009 [47], corn stover, summer squash, and tomato vine have relatively similar flow behavior, and they are categorized as “Fair flowing” materials. The soybean stalk, eggplant, and sawdust samples are classified as “Cohesive” in terms of flowability. The cucumber has the best free-flow properties, and it is categorized as “Free flowing.”

The highest and lowest specific particle density and bulk density belong to summer squash and corn stover, respectively. This result is interesting as both the highest and lowest particle and bulk density resulted in a fair flow behavior compared to other samples. The possible justification for the fair flow behavior of the ground tomato vines, Cucumber, and summer squash is their smaller particle size distribution. The findings of Xu *et al.* and Crawford *et al.* verify our results that smaller particles result in higher particle and bulk density and better flowability [42], [43]. Moreover, the possible reason to explain flow behavior of the ground corn stover though can be the high level of the extractives in this sample. Extractives contain considerable amount of waxes which can perform as a natural lubrication [54] agent in such way to enhance the flowability of the ground corn stover.

4. DISCUSSION AND CONCLUSION

The research presented in this paper focuses on the post-harvest process properties of six biomass species grown experimentally, either in the field or in the greenhouse. It provides a comprehensive study on the processing and handling properties of corn stover, soybean stalks, tomato vines, eggplant, cucumber, summer squash, and sawdust samples. The investigation of non-traditional agricultural residue provides some abundant underutilized alternative

sources of biomass but also enables us to move toward more sustainable practices in agriculture in terms of circular economy. A commercially available sawdust is used as a benchmark. The objective was to highlight the critical properties of biomass that are important to consider when developing new biomass crops. In future experiments, we recommend segregating leaves from stems to reduce the effect of leaves on the grinding and flow properties of the materials.

The following conclusions can be drawn:

- There is a wide range of energy to grind the experimental crops. The net specific energy required for comminuting the six types of biomass varied, with the lowest being 5.1 kWh/t for summer squash stalks and the highest reaching 31.7 kWh/t for soybean stalks. The NSGEC of the samples are correlated positively with the lignin content.
- The ground summer squash stalks had the smallest particle size, while the largest particle size belonged to soybean stalks.
- The ground soybean stalks showed statistically higher angle of repose and larger Hausner ratio than other ground samples ($P = 0.05$). This can contribute to its worst flowability behavior.
- The Carbon to Oxygen (C/O) ratio is a key parameter for the analysis of the physio-chemical and structural properties of the ground biomass. All studied parameters including GCV, ash, lignin, and NSGEC are correlated significantly to C/O ratio.

5. CREDIT AUTHORSHIP CONTRIBUTION STATEMENT

Omid Gholami Banadkoki: Conceptualization, Data curation, Formal analysis, Investigation, Methodology, Software, Visualization, Writing–original draft, Writing–review and editing. Shahab Sokhansanj: Conceptualization, Methodology, Project administration, Resources, Supervision, Validation, Writing–review and editing. Anthony Lau: Conceptualization, Project administration, Resources, Supervision. Jun Sian Lee: Formal analysis, Methodology, Writing–review. Selvakumari Arunachalam: Conceptualization, Methodology, Project administration, Resources. Donald Smith: Conceptualization, Methodology, Project administration, Resources.

6. DECLARATION OF GENERATIVE AI TECHNOLOGIES IN THE WRITING PROCESS

During the preparation of this research paper, the authors used ChatGPT and CoPilot tools to enhance English and readability. After using these services, the authors reviewed and edited the content as needed and will take full responsibility for the content of the publication.

APPENDIX NOMENCLATURE

| | |
|-------|---|
| MC | Moisture content, (wb, %) |
| GCV | Gross Calorific Value, (MJ/kg, db) |
| AC | Ash Content, (%) |
| PSD | Particle Size Distribution, (%) |
| D16 | 16 % of the particles have diameter less than the specific amount, (mm) |
| D50 | 50 % of the particles have diameter less than the specific amount, (mm) |
| D84 | 84 % of the particles have diameter less than the specific amount, (mm) |
| SPD | Specific Particle Density, (kg/m ³) |
| AOR | Angle of Repose, (°) |
| HR | Hausner Ratio, (—) |
| NSGEC | Net Specific Grinding Energy Consumption, (kWh/t) |
| TSGEC | Total Specific Grinding Energy Consumption (kWh/t) |
| W | Width, (mm) |
| L | Length, (mm) |
| A | Area, (mm ²) |
| P | Perimeter, (mm) |
| AR | Aspect Ratio, (—) |

ACKNOWLEDGMENT

The authors gratefully acknowledge the graduate support provided by the NSERC (#11759). The authors acknowledge Premium Pellet Co., Vanderhoof, British Columbia for providing sawdust samples. Finally, the authors extend their appreciation to Dr. Jun Sian Lee and Dr. Hamid Rezaei for their technical support.

Conflict of Interest

The authors declare that they have no known conflict of financial interests or personal relationships that could have appeared to influence the work reported in this paper.

REFERENCES

- [1] Gorjian S, Fakhraei O, Gorjian A, Sharafkhani A, Aziznejad A. Sustainable food and agriculture: employment of renewable energy technologies. *Curr Robot Rep*. 2022;3:153–63. doi: 10.1007/s43154-022-00080-x.
- [2] Branthôme. Tomato leaves, an important potential source of high quality protein? 2022. Available from: https://www.tomatonews.com/en/tomato-leaves-an-important-potential-source-of-high-quality-protein_2_1733.html. (accessed January 21, 2024).
- [3] Shahbandeh. Harvested area: tomatoes Canada. 2023. Available from: <https://www.statista.com/statistics/453607/area-of-tomatoes-harvested-in-canada/> (accessed January 21, 2024).
- [4] Kassab Z, Kassem I, Hannache H, Bouhfid R, Qaiss AEK, Achaby MEI. Tomato plant residue as new renewable source for cellulose production: extraction of cellulose nanocrystals with different surface functionalities. *Cellulose*. 2020;27:4287–303. doi: 10.1007/s10570-020-03097-7.
- [5] Undersander. Soybeans for hay or silage, crops and soils. 2023. Available from: <https://cropsandsoils.extension.wisc.edu/articles/soybeans-for-hay-or-silage/>. (accessed January 21, 2024).
- [6] Ferrer A, Salas C, Rojas OJ. Physical, thermal, chemical and rheological characterization of cellulosic microfibrils and microparticles produced from soybean hulls. *Ind Crops Prod*. 2016;84:337–43. doi: 10.1016/J.INDCROP.2016.02.014.
- [7] Bitra VSP, Womac AR, Yang YT, Miu PI, Igathinathane C, Chevanan N, et al. Characterization of wheat straw particle size distributions as affected by knife mill operating factors. *Biomass Bioenergy*. 2011;35:3674–86. doi: 10.1016/J.BIOMBIOE.2011.05.026.
- [8] Khullar E, Dien BS, Rausch KD, Tumbleson ME, Singh V. Effect of particle size on enzymatic hydrolysis of pretreated Miscanthus. *Ind Crops Prod*. 2013;44:11–7. doi: 10.1016/J.INDCROP.2012.10.015.
- [9] Oyedele O, Gitman P, Qu J, Webb E. Understanding the impact of lignocellulosic biomass variability on the size reduction process: a review. *ACS Sustain Chem Eng*. 2020;8:2327–43. doi: 10.1021/acsschemeng.9b06698.
- [10] Colley Z, Fasina OO, Bransby D, Lee YY. Moisture effect on the physical characteristics of switchgrass pellets. *Trans ASABE*. 2006;49:1845–51.
- [11] Kaliyan N, Student G, Morey RV. Morey, densification of corn stover. *Written for Presentation at the 2005 ASAE Annual International Meeting Sponsored by ASAE*, 2005.
- [12] Lv PM, Xiong ZH, Chang J, Wu CZ, Chen Y, Zhu JX. An experimental study on biomass air-steam gasification in a fluidized bed. *Bioresour Technol*. 2004;95:95–101. doi: 10.1016/j.biortech.2004.02.003.
- [13] Kulkarni A, Baker R, Abdoulmoumine N, Adhikari S, Bhavnani S. Experimental study of torrefied pine as a gasification fuel using a bubbling fluidized bed gasifier. *Renew Energy*. 2016;93:460–8. doi: 10.1016/j.renene.2016.03.006.
- [14] Dumas C, Silva Ghizzi Damasceno G, Abdellatif B, Carrère H, Steyer JP, Rouau X. Effects of grinding processes on anaerobic digestion of wheat straw. *Ind Crops Prod*. 2015;74:450–6. doi: 10.1016/J.INDCROP.2015.03.043.
- [15] Ciesielski PN, Wiggins GM, Jakes JE, Daw CS. Simulating biomass fast pyrolysis at the single particle scale. 2017. Available from: www.rsc.org.
- [16] Tian Y, Perré P. Effects of particle size on the pyrolysis of spruce and poplar: thermogravimetric analyses, DAEM modelling, validation, and prediction of secondary charring. *Biomass Bioenergy*. 2023;176:106913. doi: 10.1016/J.BIOMBIOE.2023.106913.
- [17] Jewiarz M, Wróbel M, Mudryk K, Szufa S. Impact of the drying temperature and grinding technique on biomass grindability. *Energies (Basel)*. 2020;13. doi: 10.3390/en13133392.
- [18] Moiceanu G, Paraschiv G, Voicu G, Dinca M, Negoita O, Chitoiu M, Tudor P. Energy consumption at size reduction of lignocellulose biomass for bioenergy. *Sustainability (Switzerland)*. 2019;11. doi: 10.3390/su11092477.
- [19] Liu Y, Wang J, Wolcott MP. Assessing the specific energy consumption and physical properties of comminuted Douglas-fir chips for bioconversion. *Ind Crops Prod*. 2016;94:394–400. doi: 10.1016/J.INDCROP.2016.08.054.
- [20] Naimi L, Member A, Sokhansanj S, Fellow P-A, Bi X, Lim CJ. A study on the impact of wood species on grinding performance. *Written for Presentation at the 2012 ASABE Annual International Meeting Sponsored by ASABE*, 2012.
- [21] Mckendry P. Energy production from biomass (part 1): overview of biomass. 2002.
- [22] Tan F, He L, Zhu Q, Wang Y, Hu G, He M. Characterization of different types of agricultural biomass and assessment of their potential for energy production in China. *Bioresources*. 2019;14:6447–64.
- [23] Prins MJ, Ptasiński KJ, Janssen FJJG. From coal to biomass gasification: comparison of thermodynamic efficiency. *Energy*. 2007;32:1248–59. doi: 10.1016/j.energy.2006.07.017.
- [24] Inna S, Henriette AZ, Boukar H, Cornelius T, Cârâc G, Mihaela RD, Ruben M, Richard K. Compositional characteristics and theoretical energy potential of animal droppings from Adamawa region of Cameroon. *Biomass Convers Biorefin*. 2022. doi: 10.1007/s13399-022-03320-4.
- [25] de Souza Rossin AR, da S.L. Cardoso F, Cordeiro CC, Breitenbach GL, Caetano J, Dragunski DC. Chemical properties of biomass. *Handb Biomass*. 2024;331–47. doi: 10.1007/978-981-99-6727-8_12.

- [26] Inna S, Amadou OA, Yvette JN, Cârâc G, Mihaela RD, Richard K. Assessment of efficient thermal conversion technologies and hlv from compositional characteristics of cassava peelings, plantain peelings and corn cobs. *Energy Res J*. 2022;13:30–41. doi: 10.3844/erjsp.2022.30.41.
- [27] Sun P, Wang C, Zhang M, Cui L, Dong Y. Ash problems and prevention measures in power plants burning high alkali fuel: brief review and future perspectives. *Sci Total Environ*. 2023;901. doi: 10.1016/j.scitotenv.2023.165985.
- [28] Nakashima GT, Martins MP, Hansted ALS, Yamamoto H, Yamaji FM. Sugarcane trash for energy purposes: storage time and particle size can improve the quality of biomass for fuel? *Ind Crops Prod*. 2017;108:641–8. doi: 10.1016/j.indcrop.2017.07.017.
- [29] Akowuah JO, Kemausuor F, Mitchual SJ. Physico-chemical characteristics and market potential of sawdust charcoal briquette. *Int J Energy Environ Eng*. 2012;3:1–6. doi: 10.1186/2251-6832-3-20.
- [30] Shaba Mohammed I, Aliyu M, Aliyu Abdullahi N, Ahmed Alhaji I. Production of bioenergy from rice-melon husk co-digested with cow dung as inoculant. 2020. Available from: <http://www.cigrjournal.org>.
- [31] Cheng Z, Leal JH, Hartford CE, Carson JW, Donohoe BS, Craig DA, et al. Flow behavior characterization of biomass Feedstocks. *Powder Technol*. 2021;387:156–80. doi: 10.1016/j.powtec.2021.04.004.
- [32] Hann D, Strazisar J. Influence of particle size distribution, moisture content, and particle shape on the flow properties of bulk solids. *Instrum Sci Technol*. 2007;35:571–84. doi: 10.1080/10739140701540453.
- [33] Mani S, Tabil LG, Sokhansanj S. Grinding performance and physical properties of wheat and barley straws, corn stover and switchgrass. *Biomass Bioenergy*. 2004;27:339–52. doi: 10.1016/j.biombioe.2004.03.007.
- [34] Miao Z, Grift TE, Hansen AC, Ting KC. Energy requirement for comminution of biomass in relation to particle physical properties. *Ind Crops Prod*. 2011;33:504–13. doi: 10.1016/j.indcrop.2010.12.016.
- [35] Pordesimo LO, Igathinathane C, Holt GA. Hammer milling switchgrass from weathered bales. *Ind Crops Prod*. 2023;197:116647. doi: 10.1016/J.INDCROP.2023.116647.
- [36] Chaloupková V, Ivanova T, Ekrt O, Kabutay A, Herák D. Determination of particle size and distribution through image-based macroscopic analysis of the structure of biomass briquettes. *Energies (Basel)*. 2018;11. doi: 10.3390/en11020331.
- [37] Igathinathane C, Melin S, Sokhansanj S, Bi X, Lim CJ, Pordesimo LO, et al. Machine vision based particle size and size distribution determination of airborne dust particles of wood and bark pellets. *Powder Technol*. 2009;196:202–12. doi: 10.1016/j.powtec.2009.07.024.
- [38] Michalska-Požoga I, Tomkowski R, Rydzkowski T, Thakur VK. Towards the usage of image analysis technique to measure particles size and composition in wood-polymer composites. *Ind Crops Prod*. 2016;92:149–56. doi: 10.1016/J.INDCROP.2016.08.005.
- [39] Rezaei H, Sokhansanj S. Physical and thermal characterization of ground bark and ground wood particles. *Renew Energy*. 2018;129:583–90. doi: 10.1016/j.renene.2018.06.038.
- [40] Rezaei H, Lim CJ, Lau A, Sokhansanj S. Size, shape and flow characterization of ground wood chip and ground wood pellet particles. *Powder Technol*. 2016;301:737–46. doi: 10.1016/j.powtec.2016.07.016.
- [41] Igathinathane C, Pordesimo LO, Columbus EP, Batchelor WD, Methuku SR. Shape identification and particles size distribution from basic shape parameters using ImageJ. *Comput Electron Agric*. 2008;63:168–82. doi: 10.1016/j.compag.2008.02.007.
- [42] Xu G, Li M, Lu P. Experimental investigation on flow properties of different biomass and torrefied biomass powders. *Biomass Bioenergy*. 2019;122:63–75. doi: 10.1016/j.biombioe.2019.01.016.
- [43] Crawford NC, Nagle N, Sievers DA, Stickel JJ. The effects of physical and chemical preprocessing on the flowability of corn stover. *Biomass Bioenergy*. 2016;85:126–34. doi: 10.1016/J.BIOMBIOE.2015.12.015.
- [44] Tannous K, Lam PS, Sokhansanj S, Grace JR. Physical properties for flow characterization of ground biomass from douglas fir wood. *Particulate Sci Technol*. 2013;31:291–300. doi: 10.1080/02726351.2012.732676.
- [45] Shah RB, Tawakkul MA, Khan MA. Comparative evaluation of flow for pharmaceutical powders and granules. *AAPS Pharm-SciTech*. 2008;9:250–58. doi: 10.1208/s12249-008-9046-8.
- [46] Littlefield B, Fasina OO, Shaw J, Adhikari S, Via B. Physical and flow properties of pecan shells-Particle size and moisture effects. *Powder Technol*. 2011;212:173–80. doi: 10.1016/j.powtec.2011.05.011.
- [47] McGlinchey D. *Bulk Solids Handling: Equipment Selection and Operation*. Blackwell Pub; 2008.
- [48] Ulusoy U, Yekeler M, Hıçılmaz C. Determination of the shape, morphological and wettability properties of quartz and their correlations. *Miner Eng*. 2003;16:951–64. doi: 10.1016/j.mineng.2003.07.002.
- [49] Geldart D, Abdullah EC, Hassanpour A, Nwoke LC, Wouters I. Characterization of powder flowability using measurement of angle of repose. *China Particuology*. 2006;4:104–7.
- [50] Sluiter A, Hames B, Ruiz R, Scarlata C, Sluiter J, Templeton D. Determination of ash in biomass: laboratory analytical procedure (LAP); Issue Date: 7/17/2005. 2008. Available from: www.nrel.gov.
- [51] Sluiter A, Hames B, Ruiz R, Scarlata C, Sluiter J, Templeton D, et al. Determination of structural carbohydrates and lignin in biomass laboratory analytical procedure (LAP) Issue Date: 7/17/2005. 2008.
- [52] Karinkanta P, Ämmälä A, Illikainen M, Niinimäki J. Fine grinding of wood—Overview from wood breakage to applications. *Biomass Bioenergy*. 2018;113:31–44. doi: 10.1016/j.biombioe.2018.03.007.
- [53] Widyorini R, Xu J, Watanabe T, Kawai S, Widyorini R, Xu J, et al. Chemical changes in steam-pressed kenaf core binderless particleboard. *J Wood Sci*. Springer, 2005;51(2003):26–32. doi: 10.1007/s10086-003-0608-9.
- [54] Oleson KR, Schwartz DT. Extractives in Douglas-fir forestry residue and considerations for biofuel production. *Phytochem Rev*. 2016;15:985–1008. doi: 10.1007/S11101-015-9444-Y/TABLES/16.